J. Membrane Biol. 143, 19–28 (1995)

The Journal of
Membrane
Biology

Transport and Dynamics of Molecules Dissolved in Maize Root Cortex Membranes

J. Svetek[1], V. Furtula[2], M. Nemec[1], E.A. Nothnagel[2], M. Schara[1]

[1]J. Stefan Institute, University of Ljubljana, 61111 Ljubljana, Jamova 39/p.p. 100/, Slovenia
[2]Department of Botany and Plant Sciences, University of California, Riverside, California 92521

Received: 15 March 1994/Revised: 9 September 1994

Abstract. Translational diffusion of a fluorescent sterol probe was measured in the plasma membranes of protoplasts isolated from cortical cells of the primary root of maize seedlings. The apparent lateral diffusion coefficient was typically observed to be nearly insensitive to temperature, while the mobile fraction increased with increasing temperature. These fluorescence photobleaching recovery (FPR) measurements were compared with the electron paramagnetic resonance (EPR) spectra of the methyl ester of 13-doxyl palmitic acid in membranes of corn root tissue *in situ*. The complex spectra observed with this probe were analyzed as weighted sums of simpler spectra of various order parameters and rotational correlation times. The reconstituted spectra calculated from the model show that EPR also detects a mobile (less ordered, fluid) fraction, distinguished by the order parameter $S = 0.1$ to 0.2, which becomes more abundant as temperature increases and is qualitatively comparable to the mobile fraction determined by the FPR method. The observed results on the mobile fractions and the diffusion rates for translational (FPR) as well as rotational (EPR) motions are interpreted in terms of membrane organization, thus providing information on the population and structural patterns of the coexisting domains with a special emphasis on the response of the membrane to temperature changes.

Key words: Plant membrane — Lipid domain — Fluorescence photobleaching recovery — Electron paramagnetic resonance — Temperature stress — *Zea mays*

Introduction

The strategic position and structure of the membranes in cells infer their direct or indirect involvement in a wide range of processes in tissues. Within this range of membrane processes, the role of membranes in the response of cells or tissues to temperature stress is an area of considerable interest for a wide variety of organisms. Temperature effects on membranes are conveniently studied by a variety of biophysical techniques, but results obtained with different techniques applied to the same biological system are not always consistent. While such inconsistencies confound data interpretation, they also emphasize the value of using more than one technique to assess the role of membranes in biological responses to temperature stress [30].

Apparent inconsistencies in data from different biophysical techniques can sometimes be rationalized on the basis of probe location. For example, one technique might involve use of a probe molecule that localizes in the polar head region of a membrane, while another technique involves use of a probe that localizes in the hydrophobic midplane. Similarly, some techniques, such as electron paramagnetic resonance (EPR), nuclear magnetic resonance, and fluorescence depolarization, are inherently most sensitive to short-range molecular motions, while other techniques, such as fluorescence photobleaching recovery (FPR), assess motions over distances much longer than molecular dimensions. Theoretical models relating long- and short-range motions are not always reliable as discussed previously [10, 26].

The present work involves the combined application of a long-range technique (FPR) and a short-range technique (EPR) to assess heterogeneity of molecular motions *in situ* in membranes of live cells and tissue. The model system is the cortical tissue of the primary root of maize seedlings, and the approach is enhanced by the comparison of genotypes that differ in chilling sensitivity. In our previous work [23], we found that molecular transport across the cellular membranes exhibited some genotypic differences that might be related to chilling resistance. More generally, the importance of the lipid phase state relative to plant chilling sensitivity [9] con-

Correspondence to: M. Schara

tinues to be supported by an increasing body of evidence, including the recent demonstration that chilling resistance of tobacco is influenced by genetically engineered changes in the degree of unsaturation of fatty acids in the phosphatidyl glycerol of chloroplast membranes [16].

Materials and Methods

Plant Material

Maize (*Zea mays* L.) seeds were obtained from the Maize Research Institute, Belgrade, Yugoslavia. Three genotypes that differ in chilling sensitivity (L. Zarić, S. Pekić, B. Kerečki, and L. Satarić; Maize Research Institute, *unpublished* data) were used: K-33 (chilling sensitive). BCL-48 (chilling resistant) and F-2 (intermediate). The seeds were germinated on wet filter or blotting paper in the dark for 4 days at 25°C, and then the root cortex was separated from the stele as described [8]. The resulting cortical sleeves were either used for the EPR experiments or for the isolation of protoplasts for the FPR experiments. Protoplast isolation was done at 25°C according to Gronwald and Leonard [8], except that the mannitol concentration was lowered to 0.45 M [6].

Fluorescence Labeling and FPR Measurements

The fluorescent probe, a Lucifer Yellow conjugate of cholesterol (LY-Chol), was synthesized as described [17]. Protoplasts were labeled for 20 min at 25°C with 0.1 mg/ml (0.115 mM) LY-Chol and then washed [6]. Fluorescence photobleaching recovery (FPR) measurements were performed with an instrument and methods previously described [5, 18]. The radius of the laser beam at focus on the specimen was periodically measured [29] during the course of the investigation and was always within the range of 0.550 to 0.783 μm, i.e., the smallest laser spot that could be focused with a given microscope objective lens (40×). A slightly smaller beam could be obtained by using a 100× lens, but it would require oil immersion and thus thermal contact with the specimen which would disturb our temperature variation measurements. Curve-fitting to obtain the apparent lateral diffusion coefficient (D) and mobile fraction (M) was based on the theoretical models of Axelrod et al. [3]. The values for D and M reported in the figures are averages ± SD of 4 to 14 values, each obtained by analyzing the average of 10 individual diffusion curves recorded from protoplasts isolated in at least two different batches. Temperature control in the range of 1.7 to 37°C was achieved during FPR measurements by using a water-jacketed microscope stage connected to a circulating bath. Specimen temperature was measured with a miniature thermocouple bonded to the top of the microscope slide. As has been typically observed in many other studies of lateral diffusion of plasma membrane components in either animal or plant cells, the D and M values determined in the present study exhibited considerable variation within the population of cells. To facilitate identification of statistically significant differences in compared values, analysis of variance and the Student-Newman-Keuls post test of significance were performed with the assistance of the InStat program (GraphPad Software, San Diego, CA) for personal computers. Tabulated activation energies were calculated from the results of linear regression analyses performed with the same program.

Spin Labeling and EPR Measurements

Ten microliters of a 0.01 M ethanolic solution of the spin probe, methyl ester of 13-doxyl palmitic acid (MeFASL(2,11)), was added to 1 ml of phosphate buffered saline (PBS, pH 7.4, osmolality 310 mmol/kg). The root cortex was immersed in this solution for 30 min at room temperature, subsequently rinsed with PBS, briefly dried by blotting on filter paper, halved along the root axis, and finally put into a 1 mm inner diameter glass capillary. Only the portion of the cortex closest to the tip of the root, about 1 cm long, was used for EPR measurements in the temperature range between 5 and 35°C, using a Bruker ESP 300 X-band spectrometer equipped with a Eurotherm temperature controller.

Complex line-shapes of the EPR spectra were analyzed through reconstruction from weighted contributions of typical spectral components arising from spin-labeled molecules dissolved in different environments representing the coexisting lipid domains in the membrane. In view of the spin probe used and the position of its doxyl group within the central region of the membrane bilayer, the experimental spectra were fitted by the calculated spectra through use of a model based on rapid motion of the nitroxide in membranes and axial symmetry of the magnetic coupling tensors (g and A) [7]. The method has been described in detail elsewhere [35].

It is noted that EPR measurements on protoplasts were unsuccessful because protoplast suspensions of sufficient concentration could not be obtained. It is also noted that the pre-eminent considerations in lipid probe selection were proper and reliable membrane insertion and retention, rather than structural similarity between the FPR and EPR probes. Thus, LY-Chol was selected because it readily labels the maize protoplast plasma membrane and maintains a high ratio of cell surface-to-cytoplasmic fluorescence [17], while MeFASL(2,11) was selected because it readily overcomes the cell wall barrier and achieves reliable and sufficient membrane insertion *in situ* in the maize root tissue. A fatty acid-type fluorescent probe was tested with protoplasts, and a cholestane-type spin label was tested with root cortex, but these probes exhibited poor membrane insertion and/or retention.

Abbreviations

EPR,	electron paramagnetic resonance;
FPR,	fluorescence photobleaching recovery;
MeFASL(2,11),	methyl ester of 13-doxyl palmitic acid;
LY-Chol,	dilithium 4-amino-*N*-[(β-(carbo(5-cholesten-3β-yl)-oxy)hydrazinocarbonyl)amino]-1,8-naphthalimide-3,6-disulfonate;
D,	apparent lateral diffusion coefficient;
M,	mobile fraction;
SD,	standard deviation,
PBS,	phosphate buffered saline;
S,	order parameter,
τ,	rotational correlation time;
W,	relative EPR intensity weighting factor;
ΔE,	Arrhenius activation energy.

Results

Lateral Diffusion Parameters Determined by FPR

Apparent lateral diffusion coefficients (D) of the sterol probe LY-Chol in the plasma membrane were in the range of (1 to 5) × 10^{-9} cm^2/sec for all three genotypes and exhibited little, if any, dependence on temperature (Figs. 1*A*, 2*A*, 3*A*). Analysis of variance for between-temperature comparisons of D in BCL-48 showed no

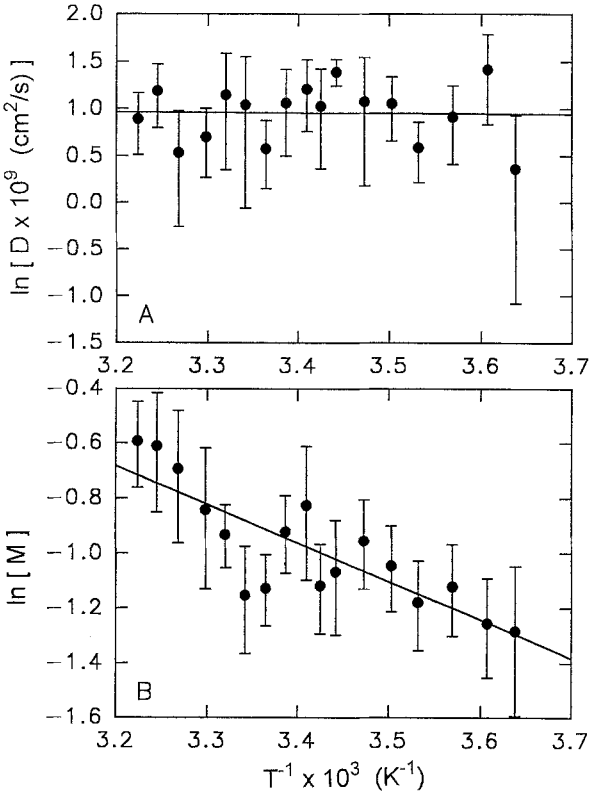

Fig. 1. Temperature dependence of lateral diffusion of the LY-Chol sterol probe in the plasma membrane of BCL-48 maize protoplasts. The apparent diffusion coefficient (*A*) and mobile fraction (*B*) were determined by the FPR technique. Plotted points are averages with ± SD error bars, and continuous lines are least squares fits to the averages at the temperatures across the entire 1.7 to 37°C range.

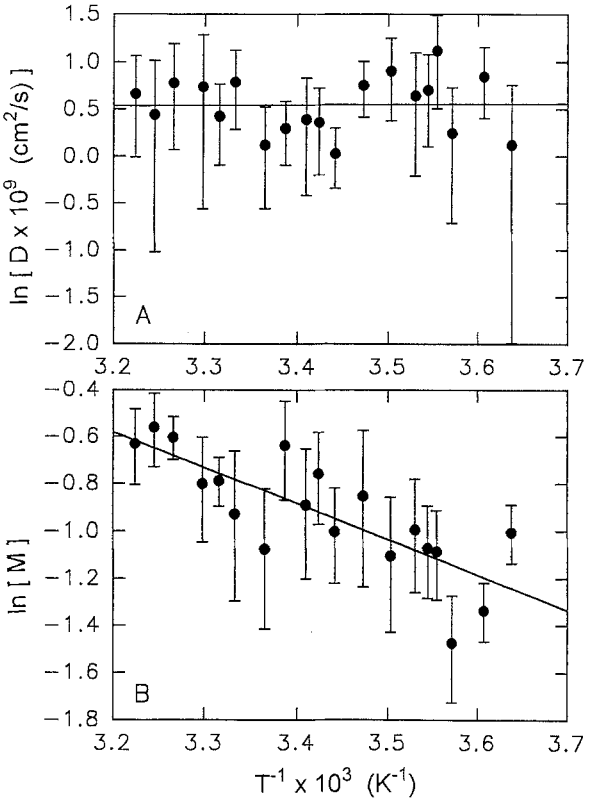

Fig. 2. Temperature dependence of lateral diffusion of the LY-Chol sterol probe in the plasma membrane of F-2 maize protoplasts. Other details as in Fig. 1.

significant differences except for a few pairs involving either 1.7 or 4.1°C. Likewise, between-temperature comparisons of *D* in F-2 showed no significant differences except for a few pairs involving 8.2°C. Linear regression analysis of the temperature dependence of *D* in Arrhenius format yielded slopes that were not significantly different from zero for either BCL-48 or F-2 (Table 1). When averaged across the temperature range and compared, however, the *D* values for BCL-48 ((2.63 ± 0.24) × 10^{-9} cm^2/sec, mean and 95% C.I.) and F-2 ((1.76 ± 0.18) × 10^{-9} cm^2/sec) were highly significantly different ($P < 0.001$). In partial contrast to the results for the BCL-48 and F-2 genotypes, *D* for K-33 (Fig. 3*A*) did show some limited trends with temperature. An increase of *D* with increasing temperature occurred in the 22 to 37°C range, and a linear regression analysis restricted to this temperature region (dashed line in Fig. 3*A*) yielded a slope that was significantly different from zero ($P = 0.013$) and indicated no significant departures from linearity. The corresponding Arrhenius activation energy was 21.7 ± 17.0 kJ/mol (mean and 95% C.I.). At lower temperatures, *D* exhibited an unexpected but significant increase, coupled with an anomaly between 10 and 17°C. Due to these larger *D* values at lower temperatures, a single linear regression analysis over the entire 1.7 to 37°C range yielded a negative activation energy (Table 1) but indicated very significant departures from linearity. Overall, however, the variation of *D* with temperature between 1.7 and 37°C was quite modest for K-33. When averaged across this temperature range, *D* for K-33 ((1.64 ± 0.14) × 10^{-9} cm^2/sec) was not significantly different from *D* of F-2 but was highly significantly different from *D* of BCL-48 ($P < 0.001$).

Mobile fractions (*M*) of the sterol probe LY-Chol in the plasma membrane were in the range of 0.23 to 0.57 for all three genotypes and exhibited overall increases within this range as temperature increased from 1.7 to 37°C (Figs. 1*B*, 2*B*, 3*B*). The remaining fraction of the sterol probe moved so slowly that it appeared immobile on the time scale (typically 8 sec) of the experiment. With the data expressed in Arrhenius format, a single linear regression for each genotype was performed over the entire 1.7 to 37°C temperature range. Although this analysis indicated that significant departures from linearity occurred for each genotype, the appearance of the data (Figs. 1*B*, 2*B*, 3*B*) did not convince us that a more complex analysis was warranted. The Arrhenius activation energies resulting from the simple linear regressions

Table 1. Summary of temperature variations of translational and rotational motions of labeled molecules in maize root cell membranes

Parameter	Genotype			Refers to
	BCL-48	F-2	K-33	
FPR data from protoplasts				
$D_{20} \times 10^9$ (cm^2/sec)	3.4 ±1.3	1.5 ±0.7	1.3 ±0.3	Figs. 1*A*–3*A*
ΔE_D (kJ/mol)	3.1 ±6.3	2.3 ±7.6	−11.1 ±5.7*	Figs. 1*A*–3*A*
M_{20}	0.44 ± 0.11	0.41 ± 0.09	0.31 ± 0.04	Figs. 1*B*–3*B*
ΔE_M (kJ/mol)	11.7 ±2.3*	11.5 ±3.1*	5.9 ±2.3*	Figs. 1*B*–3*B*
EPR data from root tissue				
τ_{20} (NS)	1.2 ±0.2	ND	1.3 ±0.2	Tab. 2, component (*c*)
ΔE_τ (kJ/mol)	6.6 ±5.8	ND	9.1 ±2.9	Fig. 6
W_{c20}	0.40 ± 0.07	ND	0.46 ± 0.08	Tab. 2
ΔE_{W_c} (kJ/mol)	3.0 ±1.8	ND	20.8 ±2.9	Fig. 7

The value of each parameter at 20°C is listed, together with its Arrhenius activation energy as estimated from a single linear regression analysis of all repeated determinations at all temperatures examined. Error ranges are 95% confidence intervals.
* ΔE is highly significantly different from zero ($P < 0.001$). Other ΔE for FPR data are not significantly different from zero. ND = not determined.

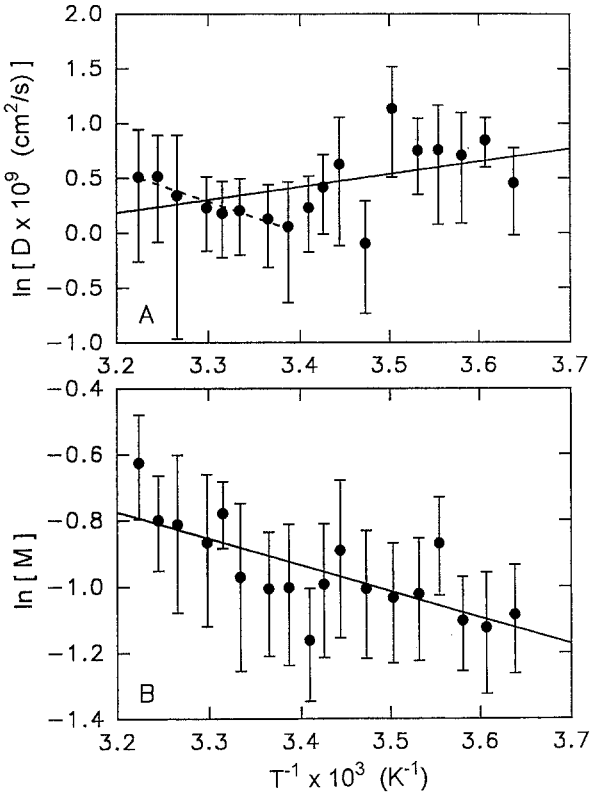

Fig. 3. Temperature dependence of lateral diffusion of the LY-Chol sterol probe in the plasma membrane of K-33 maize protoplasts. Other details as in Fig. 1, except the dashed line in *A*, which is a least squares fit restricted to the 22 to 37°C range.

were all positive and highly significantly different from zero (Table 1). These *M* activation energies did not differ significantly between BCL-48 and F-2, but the value for K-33 was only about half as large.

Since the F-2 genotype did not exhibit any unique lateral diffusion parameters that were strikingly different from those exhibited by either BCL-48 or K-33, our continuing studies were limited to a comparison of the BCL-48 and K-33 genotypes, these representing the extremes among the chilling sensitivities of the three genotypes.

At this point it is worth mentioning that some contribution to these mobile fraction changes with temperature might in principle be ascribed to alterations of the individual membrane domain sizes relative to the laser spot size [34]. The EPR results presented in the next subsection and compared with FPR in the Discussion, however, strongly indicate that the prevalent contribution to the temperature variations of the FPR mobile fraction stems from relative changes in the overall cell membrane area fraction populated by the fluid domains.

Evaluation of the EPR Spectra

The observed complex EPR spectra were evident superimpositions of several simpler spectra arising from spin probe molecules distributed within membrane regions with different ordering and dynamics of their molecular constituents (Figs. 4, 5). The spectra calculated as contributions from different membrane regions were characterized by different order parameters *S* and rotational correlation times τ (Table 2). The best calculated fits to two typical experimental spectra are shown in Fig. 4. The four components by which the low temperature spectrum of Fig. 4*B* was reconstructed are, properly weighted, presented in Fig. 5. The parameters that produced the best reconstructions for all the other spectra are given in Table 2. The EPR intensity weighting factors *W* are directly proportional to the relative population of the membrane regions by the spin probe molecules and are thus assumed to represent the relative fractions of the membrane surface area occupied by domains with distinct ordering and dynamics of their constituents.

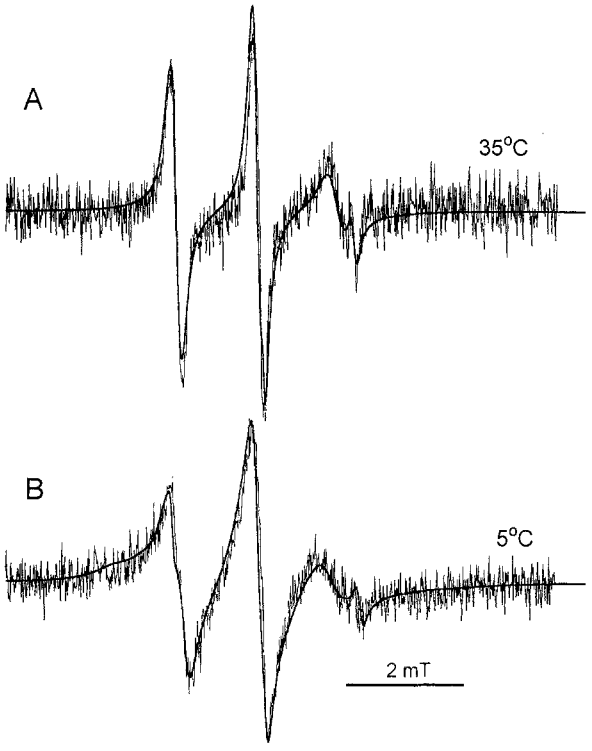

Fig. 4. Experimental spectra (noisy lines) of MeFASL(2,11) in the cell membranes of K-33 corn root tissue measured at (*A*) 35°C and (*B*) 5°C with the corresponding calculated spectra (continuous lines). In this presentation the amplitude of the spectra in *A* are diminished by a factor of three. The parameters used to calculate the spectra by the model are given in Table 2 and $A\| = 3.3$ mT, $A_\perp = 0.605$ mT, $g\| = 2.00270$ and $g_\perp = 2.00745$. The measurement of each experimental spectrum samples over about 10^7 to 10^8 cells in the root tissue.

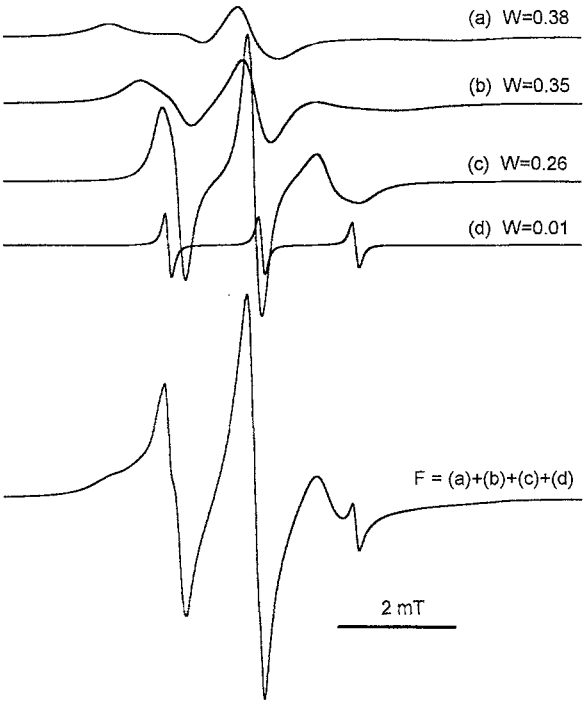

Fig. 5. Calculated spectrum F (continuous line in Fig. 4*B*) is a superimposition of four components (a, b, c, d), which are presented with the appropriate weight factors, *W*, for this particular spectrum (in Table 2 average values are listed). Components (*a*) and (*b*) are the more ordered membrane fractions, and component (*c*) represents the fluid, low ordered fraction. Component (*d*), represented by the isotropic spectrum, is present only in a minute amount (1–2%) and, due to its large hyperfine splitting (a = 1.616 mT, g = 2.00537), corresponds to the spin probe molecules in the aqueous compartments of the tissue. Other parameters used in the calculation are given in Table 2 for the spectrum of K-33 genotype measured at 5°C.

The temperature dependencies of the rotational correlation time of the spin probe molecules dissolved in fluid membrane regions of least ordering (spectral component (*c*), order parameter *S* between 0.1 and 0.2) for the genotypes BCL-48 and K-33 are shown in Fig. 6. Similar Arrhenius plots for the weighting factors of this component (less ordered, fluid component W_c) are given in Fig. 7. The corresponding activation energies derived from the semilog plots in Figs. 6 and 7 are presented in Table 1.

Analysis of the complex EPR spectra as the weighted superimpositions of several simpler spectra shows that the primary change with temperature increase from 5 to 35°C is a gradual increase in the proportion of less ordered regions of the membrane (Fig. 7), while their ordering (expressed as order parameter *S*) undergoes relatively small alterations over the same temperature range, implying that the line-shapes of the individual spectral components do not change significantly within the measured temperature range. This observation justifies the assumption that temperature variations of the weighting factors *W* directly represent changes in the relative proportions of the coexisting membrane domains. With temperature decrease, the chilling sensitive genotype K-33 exhibited a drastic increase of the immobilized, ordered membrane fractions. Over the same temperature range, the chilling resistant genotype BCL-48 exhibited much smaller changes in the relative proportions of the membrane domain fractions.

Discussion

Plant cell membrane dynamics were studied through two independent methods that assessed either lateral diffusion (FPR) or rotational diffusion (EPR) of lipid probes in the membrane. Regardless of the different time scales of the FPR and EPR measurements, it is evident that they are both selective enough to distinguish between coexisting membrane domains that differ in mobility and ordering of their molecular constituents. The present data from both techniques show that lipid domains of different molecular mobility are coexisting in the maize membranes at all temperatures studied. Application of these

Table 2. Parameters evaluated to obtain the best fit between the experimental and calculated EPR spectra of MeFASL(2,11) in membranes *in situ* in the root tissue of two maize genotypes

Genotype	T °C	Spectral component	W[1]	S[2]	τ[3] ns	γ[4] mT	$\kappa^{4,5}$	$\kappa^{8,6}$
BCL-48	5	a	0.35	0.65	3.0	0.36	1	1
		b	0.30	0.38	2.5	0.27	1	1
		c	0.34	0.15	1.2	0.17	1.08	0.9999
		d	0.01	0.02	0.001	0.09	0.93	1.0002
	10	a	0.50	0.80	3.0	0.40	1	1
		b	0.16	0.40	1.5	0.35	1	1
		c	0.33	0.20	1.0	0.22	1.08	0.9999
		d	0.01	0.02	0.001	0.08	0.93	1.0002
	15	a	0.30	0.50	3.0	0.38	1	1
		b	0.30	0.30	1.5	0.35	1	1
		c	0.38	0.15	1.5	0.20	1.10	0.9999
		d	0.02	0.02	0.001	0.09	0.94	1.0004
	20	a	0.29	0.50	3.0	0.38	1	1
		b	0.29	0.30	2.0	0.35	1	1
		c	0.40	0.15	1.2	0.20	1.08	1
		d	0.02	0.02	0.001	0.09	0.94	1.0003
	25	a	0.31	0.60	3.0	0.38	1	1
		b	0.31	0.30	3.0	0.30	1	1
		c	0.36	0.15	0.9	0.15	1.08	1
		d	0.02	0.02	0.001	0.09	0.95	1.0004
	35	a	0.30	0.60	3.0	0.38	1	1
		b	0.29	0.3	3.0	0.30	1	1
		c	0.38	0.10	0.9	0.15	1.09	0.9999
		d	0.03	0.02	0.001	0.09	0.93	1.0002
K-33	5	a	0.37	0.80	3.0	0.40	1	1
		b	0.39	0.40	2.5	0.37	1	1
		c	0.23	0.18	1.3	0.18	1.08	0.9999
		d	0.01	0.02	0.001	0.09	0.93	1.0003
	10	a	0.36	0.80	3.0	0.38	1	1
		b	0.30	0.35	2.5	0.35	1	1
		c	0.33	0.16	1.5	0.17	1.08	0.9999
		d	0.01	0.02	0.001	0.09	0.95	1.0003
	15	a	0.33	0.80	3.0	0.38	1	1
		b	0.28	0.45	2.0	0.35	1	1
		c	0.38	0.15	1.5	0.18	1.08	0.9999
		d	0.01	0.02	0.001	0.08	0.98	1.0003
	20	a	0.26	0.50	3.0	0.35	1	1
		b	0.27	0.35	2.5	0.30	1	1
		c	0.46	0.10	1.3	0.15	1.08	0.9997
		d	0.01	0.02	0.001	0.07	0.93	1.0003
	25	a	0.26	0.55	3.0	0.37	1	1
		b	0.30	0.32	2.7	0.30	1	1
		c	0.42	0.12	1.2	0.15	1.07	0.9998
		d	0.02	0.02	0.001	0.08	0.95	1.0003
	30	a	0.18	0.40	3.0	0.35	1	1
		b	0.23	0.30	2.0	0.30	1	1
		c	0.56	0.10	1.0	0.13	1.06	0.9998
		d	0.03	0.02	0.001	0.07	0.96	1.0001
	35	a	0.15	0.60	3.0	0.35	1	1
		b	0.23	0.30	2.0	0.30	1	1
		c	0.59	0.1	1.0	0.13	1.05	0.9998
		d	0.03	0.02	0.001	0.07	0.96	1.0002

These evaluated parameters correspond to the central part of the membrane lipid bilayer probed by MeFASL(2,11) where the nitroxide is attached to the carbon atom at position 13 of the palmitic acyl chain. Average parameter values obtained from the fittings of two or three spectra are listed. The measured spectra are quite reproducible, and they can be fitted using the parameter values within SD of about ±15%.

[1] EPR intensity weighting factors proportional to the surface area of membrane domains represented by different spectral components (a, b, c, d). [2] Order parameter. [3]Rotational correlation time. [4]Line-width of the individual Lorentz function. [5,6]Polarity correction factors for the magnetic coupling tensors *A* and *g*. The original values of the *A* and *g* tensor components are given in the caption to Fig. 4.

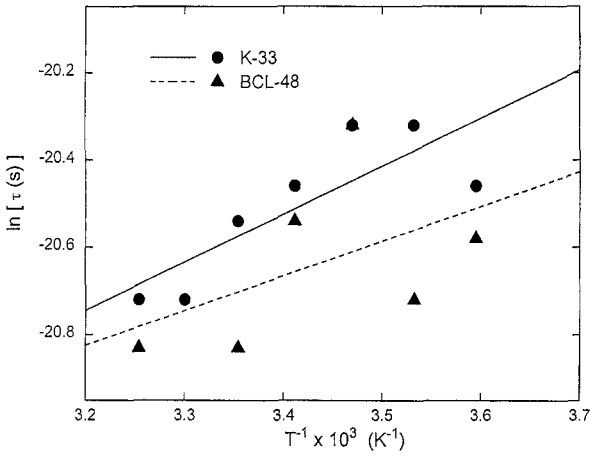

Fig. 6. Temperature dependence of the rotational correlation time τ for the fluid, less ordered spectral component (*c*) (Table 2) in the spectra of MeFASL(2, 11) measured in the cell membranes *in situ* in corn root tissue for the two genotypes K-33 and BCL-48. The rotational correlation times were evaluated as the best fits to the line-shape of the experimental spectra.

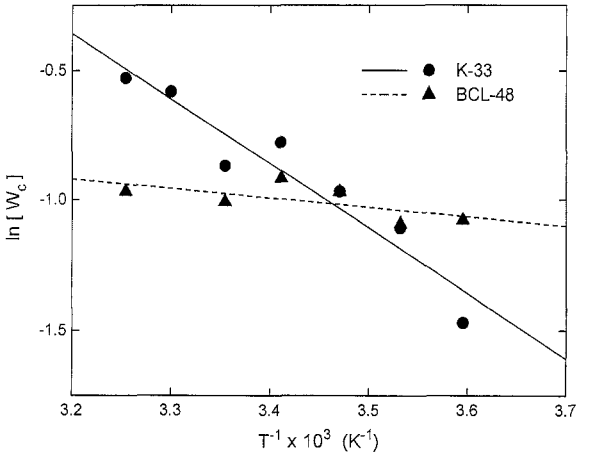

Fig. 7. Temperature dependence of the less ordered membrane fraction, W_c, represented as the weight factors of the spectral component (*c*) with the order parameter $S = 0.1$ to 0.2 in Table 2, for the spectra of MeFASL(2,11) in the cell membranes *in situ* in corn root tissue measured for the two genotypes, K-33 and BCL-48.

two fundamentally different techniques to one plant tissue in the present work has produced data that combine to strongly support and extend previous studies where separate applications of FPR [5, 6, 13, 15, 27, 29] or EPR [4, 32] led to data suggesting the existence of lipid domains in plant plasma membranes.

The fluid, less ordered membrane fraction W_c (Fig. 7), representing component (*c*) of the superimposed EPR spectrum (Table 2), can be qualitatively compared with the mobile fraction M detected by FPR (Figs. 1*B*, 3*B*). Both of them are growing in size with increasing temperature, and the proportions of the remaining, more-ordered components are correspondingly diminished. Quantitative comparison of the FPR and EPR results is fraught with difficulties, however, and the presence of domains especially complicates the interpretation of the FPR results. Thus, further interpretation of the results is somewhat more straightforward for EPR than for FPR.

The EPR technique provides a view of the molecular ordering and rotation in each domain. Rotational correlation times [25] of the MeFASL(2,11) spin probe, which are assumed to reflect environmental fluctuations by which the configurational barriers of the spin probe molecules can be crossed, describe the fast rotational molecular motion. The rotational diffusion rates and corresponding Arrhenius activation energies observed in the present work (Table 1) are qualitatively within the temperature behavior expected on the basis of many previous EPR studies of biological membranes. Since it is reasonable to assume that the spin probe concentration is equalized throughout the lipid parts of the membrane, the weighting factors W provide a good measure of the relative amount of spin probe molecules in each type of domain. Though the actual size of individual domains is not accessible by the EPR approach, the measurements on both genotypes clearly reveal the existence of both disordered, fluid domains with typical rotational motions and more ordered, rigid domains with slower rotational motions. Across the range of studied temperatures, the rotational motions in the disordered, fluid domains in K-33 tend to be slightly slower and exhibit a faster decrease with falling temperature than in BCL-48 (Fig. 6). The characteristic of K-33 having a less dynamic membrane at lower temperatures is especially apparent in the much larger activation energy of the weighting factor for the disordered, fluid domains with this genotype than with BCL-48 (Fig. 7).

In addition to changes in fluidity and ordering imposed by the membrane domain formation, as detected by EPR, compressibility might be another important characteristic of the plasma membrane associated with plant chilling resistance [14, 33]. Optimal regulation of these physical properties at the cell membrane level may have physiological relevance, especially with regard to providing proper environment for functioning of membrane-bound enzymes and for regulating the passive transport of water [24] and other molecules across cellular membranes.

The interpretation of the FPR results is immediately complicated by lateral diffusion coefficients that lack significant temperature effects, as with the BCL-48 and F-2 genotypes, or even exhibit an overall negative activation energy, as with the K-33 genotype (Table 1). These results are clearly at odds with the hydrodynamics of free lateral diffusion of molecules in thermotropic liquid crystals [20], for which positive activation energies of 20 to 40 kJ/mol are typical [11]. The observed results for maize membranes imply the action of

other effects that compensate or overwhelm the expected increase of the diffusion coefficient with temperature. We think it likely that these other effects arise because lateral diffusion in the fluid domains is not free but rather is constricted by the presence of obstacles, these being the rigid lipid domains and/or membrane proteins and protein aggregates. Thus, the measured lateral diffusion coefficients are not true diffusion coefficients but rather are apparent diffusion coefficients that reflect the effects of obstacles in the path of lipid diffusion.

The works of Saxton [21, 22] and Almeida et al. [1] present some of the recent refinements of theoretical models that have been formulated to describe lateral diffusion of membrane lipids in the presence of obstacles. Various experimental approaches to this problem have also been reported, and especially relevant to the present discussion are recent studies on lateral diffusion and fluid domain connectivity in two-phase lipid bilayers [1, 2, 28]. Based on these previous theoretical and experimental studies, at least two effects can be considered as possible mechanisms behind the steady or increasing apparent diffusion coefficients observed with decreasing temperatures in the present work on maize membranes.

One potentially important effect involves the percolation limit in two-phase lipid bilayers [1, 2, 28]. At temperatures above the percolation limit, the solid domain exists as islands in a fully connected fluid domain. As temperature drops, the solid domain islands grow at the expense of the fluid domain and coalesce until, at the percolation limit, the solid domain islands connect and become continuous while the fluid domain disconnects into pools. Using FPR and a fluorescent lipid probe that partitioned only into the fluid domain of a two-phase lipid bilayer, Almeida et al. [1, Fig. 3 therein] demonstrated that the apparent diffusion coefficient markedly decreased as the temperature was lowered toward the percolation limit. In this temperature range, the apparent diffusion rate slowed due to the obstacle effect of the growing proportion of solid domain. Once the percolation limit was reached, however, the apparent diffusion coefficient increased with further decrease in temperature. This increase in apparent diffusion rate with decreasing temperature occurred because the only type of diffusion observable by FPR was the unobstructed diffusion that occurred within fluid domain pools that were located at the edge of the illuminated spot, partially in the dark and partially in the light [1]. While the increase in apparent diffusion coefficient that we observed with decreasing temperature below 22°C in K-33 maize might involve a similar mechanism, we did not observe a precipitous drop in mobile fraction that would be characteristic of passage through a percolation limit [1, 2, 28]. This implies that, most probably, the membrane domain structure was above the percolation threshold for both genotypes even at the lower edge of the temperature range applied in our measurements.

Therefore, a second effect found in earlier studies may be a more likely mechanism behind the steady or increasing apparent diffusion coefficients observed with decreasing temperatures in the present work. Several different theoretical treatments of the obstacle problem have shown that the apparent decrease in diffusion coefficient depends on obstacle size [1, 21, 22]. Specifically, if the total obstacle area fraction of the membrane is held constant, then the apparent diffusion coefficient is significantly larger in the presence of a few large obstacles than in the present of many small obstacles. If obstacles in the maize membranes steadily coalesce as the temperature decreases, then this effect might compensate the expected decrease in the free diffusion coefficient. The obstacles might be small rigid lipid domains that coalesce into larger domains. Alternatively, the coalescing obstacles might be membrane proteins. Since many membrane proteins tend to be excluded from rigid domains [19], the protein concentration in the fluid domains of maize protoplasts might be especially high. Protein aggregation in the plasma membrane of protoplasts has been observed, in fact, by freeze fracture electron microscopy [31]. Membrane proteins coupled to the fluctuations of the cytoskeleton network should also be considered in this context [12].

Acting separately or in concert, these two effects in BCL-48 membranes might compensate the expected decrease in apparent diffusion coefficient at lower temperatures. If this hypothesis is correct, then a change in the action of these effects must occur around 22°C in K-33 (Fig. 3*A*) but not in BCL-48 (Fig. 1*A*). Except for an anomaly at about 15°C, the apparent diffusion coefficient in K-33 increases by approximately a factor of three as the temperature drops from 22 to 12°C. Above 22°C, the apparent diffusion coefficient increases with temperature in a manner consistent with free diffusion, although the large 95% confidence interval on the activation energy here (21.7 ± 17.0 kJ/mol) leaves uncertainty regarding significance. While this behavior around 22°C in K-33 has some of the characteristics of a percolation limit [1, 2, 28], neither the FPR mobile fraction (Fig. 3*B*) nor the EPR results (Figs. 6, 7) are supportive of such a drastic change in lipid dynamics at this temperature. A strong coalescence of membrane proteins or small rigid lipid domains below 22°C seems to remain as a viable hypothesis for the mechanism behind the increase in apparent diffusion coefficient.

On the other hand, comparison of temperature variations for the disordered (EPR) and the mobile (FPR) fraction in the K-33 membranes (the difference is just reverse, though less intense in the BCL-48 membranes, Table 1) leads us to the conclusion that the "microscopic" obstacle coalescence influencing the lateral diffusion rate, might be accompanied by rearrangements in the membrane domain pattern at a more "macroscopic" level. Low activation energy for the FPR mobile fraction

variations with temperature (5.9 kJ/mol, Table 1), compared with the corresponding value for the EPR disordered fraction (20.8 kJ/mol), indicate that at higher temperatures relatively large patches of the fluid membrane regions are inaccessible for the LY-Chol fluorescent probe (possibly surrounded by "strings" of small rigid domains), thus producing an apparently smaller FPR mobile fraction. As temperature drops these string-like structures seem to change, so that a higher portion of the fluid regions actually becomes a part of the FPR mobile fraction, despite overall decrease of this type of domain in the membrane, as detected by EPR.

In conclusion, we believe that the physiological implications of the experimental observations presented here are consistent with K-33 being more chilling sensitive than BCL-48. The K-33 membranes obviously suffer a drastic perturbation of membrane structure, as the temperature drops. Adequate adaptation of the cell to functioning at lower temperatures is not allowed without a substantial concomitant loss of the fluid membrane portion. Consequently, too many integral membrane enzymes may be displaced from the membrane environment which provides conditions for their optimal activity.

This work was supported in part by grants from the Ministry of Science and Technology of the Republic of Slovenia and the International Research Program of the U.S. Department of Agriculture (USDA-JF 814-51) to M.S., and by grants from the Competitive Grants Program of the U.S. Department of Agriculture (88-37264-3807 and 90-37264-5471) to E.A.N.

References

1. Almeida, P.F.F., Vaz, W.L.C., Thompson, T.E. 1992. Lateral diffusion and percolation in two-phase, two-component lipid bilayers: topology of the solid-phase domains in-plane and across the bilayer. *Biochemistry* **31:**7198–7210
2. Almeida, P.F.F., Vaz, W.L.C., Thompson, T.E. 1993. Percolation and diffusion in three-component lipid bilayers: effect of cholesterol on an equimolar mixture of two phosphatidylcholines. *Biophys. J.* **64:**399–412
3. Axelrod, D., Koppel, D.E., Schlessinger, J., Elson, E., Webb, W.W. 1976. Mobility measurement by analysis of fluorescence photobleaching recovery kinetics. *Biophys. J.* **16:**1055–1069
4. Caldwell, C.R., Whitman, C.E. 1987. Temperature-induced protein conformational changes in barley root plasma membrane-enriched microsomes. I. Effect of temperature on membrane protein and lipid mobility. *Plant Physiol.* **84:**918–923
5. Dugas, C.M., Li, Q., Khan, I.A., Nothnagel, E.A. 1989. Lateral diffusion in the plasma membrane of maize protoplasts with implications for cell culture. *Planta* **179:**387–396
6. Furtula, V., Khan, I.A., Nothnagel, E.A. 1990. Selective osmotic effect on diffusion of plasma membrane lipids in maize protoplasts. *Proc. Natl. Acad. Sci. USA* **87:**6532–6536
7. Griffith, O.H., Jost, P.C. 1976. Lipid spin labels in biological membranes. *In:* Spin Labeling. L.J. Berliner, editor. pp. 453–523. Academic, New York
8. Gronwald, J.W., Leonard, R.T. 1982. Isolation and transport properties of protoplasts from cortical cells of corn roots. *Plant Physiol.* **70:**1391–1395
9. Hiller, R.G., Raison, J.K. 1980. The fluidity of chloroplast thylakoid membranes and their constituent lipids: a comparative study by ESR. *Biophys. Biochim. Acta* **599:**63–72
10. Kleinfeld, A.M., Dragsten, P., Klausner, R.D., Pjura, W.J., Matayoshi, E.D. 1981. The lack of relationship between fluorescence polarization and lateral diffusion in biological membranes. *Biochim. Biophys. Acta* **649:**471–480
11. Krüger, G.J. 1982. Diffusion in thermotropic liquid crystals. *Physics Rep.* **82:**229–269
12. Kusumi, A., Sako, Y., Yamamoto, M. 1994. Confined lateral diffusion of membrane receptors as studied by single particle tracking (Nanovid microscopy). Effects of calcium-induced differentiation in cultured epithelial cells. *Biophys. J.* **65:**2021–2040
13. Leborgne, N., Dupou-Cezanne, L., Teulieres, C., Canut, H., Tocanne, J.-F., Boudet, A.M. 1992. Lateral and rotational mobilities of lipids in specific cellular membranes of *Eucalyptus gunnii* cultivars exhibiting different freezing tolerance. *Plant Physiol.* **100:** 246–254
14. Marčelja, S., Wolfe, J. 1979. Properties of bilayer membranes in the phase transition or phase separation region. *Biochim. Biophys. Acta* **557:**24–31
15. Metcalf, T.N., III, Wang, J.L., Schindler, M. 1986. Lateral diffusion of phospholipids in the plasma membrane of soybean protoplasts: evidence for membrane lipid domains. *Proc. Natl. Acad. Sci. USA* **83:**95–99
16. Murata, N., Ishizaki-Nishizawa, O., Higashi, S., Hayashi, H., Tasaka, Y., Nishida, I. 1992. Genetically engineered alteration in the chilling sensitivity of plants. *Nature* **356:**710–713
17. Nothnagel, E.A. 1989. Synthesis and characterization of fluorescent Lucifer yellow-lipid conjugates. *Biochim. Biophys. Acta* **980:**209–219
18. Nothnagel, E.A., Furtula, V., Dugas, C.M., Walko, R.M., Li, Q. 1990. Osmotic and temperature effects on lateral motion in the plasma membrane of maize protoplasts. *Stud. Biophys.* **138:**87–94
19. Platt-Aloia, K.A. 1988. Freeze-fracture evidence of stress-induced phase separations in plant cell membranes. *In:* Advances in Membrane Fluidity. Vol. 3. Physiological Regulation of Membrane Fluidity. R.C. Aloia, C.C. Curtain, and L.M. Gordon, editors. pp. 259–292. Alan R. Liss, New York
20. Saffmann, P.G., Delbruck, M. 1975. Brownian motion in biological membranes. *Proc. Natl. Acad. Sci. USA* **72:**3111–3113
21. Saxton, M.J. 1989. Lateral diffusion in an archipelago: distance dependence of the diffusion coefficient. *Biophys. J.* **56:**615–622
22. Saxton, M.J. 1994. Anomalous diffusion due to obstacles: a Monte Carlo study. *Biophys. J.* **66:**394–401
23. Schara, M., Nemec, M., Pečar, S. 1991. Microviscosity of *Zea mays* root cell membranes. *Period. Biol.* **93:**321–322
24. Schuler, I., Milon, A., Nakatani, Y., Ourisson, G., Albrecht, A-M., Benveniste, P., Hartmann, M.-A. 1991. Differential effects of plant sterols on water permeability and on acyl chain ordering of soybean phosphatidylcholine bilayers. *Proc. Natl. Acad. Sci. USA* **88:**6926–6930
25. Seelig, J. 1976. Anisotropic motion in liquid crystalline structures. *In:* Spin Labeling. L.J. Berliner, editor. pp. 373–409. Academic, New York
26. Shinitzky, M., Barenholz, Y. 1978. Fluidity parameters of lipid regions determined by fluorescence polarization. *Biochim. Biophys. Acta* **515:**367–394
27. Vaz, W.L.C. 1992. Translational diffusion in phase-separated lipid bilayer membranes. *In:* Comments on Molecular and Cellular Bio-

physics: Domains in Biological membranes. K. Jacobson, and W.L.C. Vaz, editors. Vol. 8, Numbers 1 and 2, pp. 17–36. Gordon and Breach Science Publishers, United Kingdom

28. Vaz, W.L.C., Melo, E.C.C., Thompson, T.E. 1989. Translational diffusion and fluid domain connectivity in a two-component, two-phase phospholipid bilayer. *Biophys. J.* **56:**869–876
29. Walko, R.M., Nothnagel, E.A. 1989. Lateral diffusion of proteins and lipids in the plasma membrane of rose protoplast. *Protoplasma* **152:**46–56
30. Wang, C.Y. 1990. Chilling Injury of Horticultural Crops. CRC, Boca Raton, FL
31. Wilkinson, M.J., Northcote, D.H. 1980. Plasma membrane ultrastructure during plant protoplast plasmolysis, isolation and wall regeneration: a freeze-fracture study. *J. Cell Sci.* **42:**401–415
32. Windle, J.J. 1988. A comparative spin-label study of isolated plasma membranes and plasma membranes of whole cells and protoplasts from cold-hardened and non-hardened winter rye. *Plant Physiol.* **88:**1388–1396
33. Wolfe, J. 1978. Chilling injury in plants: the role of membrane lipid fluidity. *Plant Cell Environ.* **1:**241–247
34. Yechiel, E., Edidin, M. 1987. Micrometer-scale domains in fibroblast plasma membranes. *J. Cell Biol.* **105:**755–760
35. Žel, J., Svetek, J. Črne, H., Schara, M. 1993. Effects of aluminum on membrane fluidity of the mycorrhizal fungus *Amanita muscaria. Physiol. Plant* **89:**172–176